WALL MITIGATION USING DISCRETE PROLATE SPHEROIDAL SEQUENCES FOR SPARSE INDOOR IMAGE RECONSTRUCTION

Fauzia Ahmad, Jiang Qian, and Moeness G. Amin

Radar Imaging Lab, Center for Advanced Communications
Villanova University, Villanova, PA 19085
E-mail:{fauzia.ahmad, jiang.qian, moeness.amin}@villanova.edu

ABSTRACT

Detection and localization of stationary targets behind walls is primarily challenged by the presence of the overwhelming EM signature of the front wall in the radar returns. In this paper, we address suppression of front wall clutter prior to image reconstruction for a stepped-frequency radar imaging system, when different sets of few frequency observations are available at different antennas in physical or synthetic aperture arrays. We use a dictionary based on discrete prolate spheroidal sequences to represent the wall return and employ a block sparse model to capture and subsequently remove the wall clutter at each available antenna. The proposed scheme enables sparsity-based image reconstruction techniques to effectively detect and localize behind-the-wall targets from reduced data measurements.

Index Terms— Through-the-Wall Radar Imaging, DPSS, Compressive Sensing, Wall Mitigation, Sparse Reconstruction.

1. INTRODUCTION

Detection and localization of stationary targets inside enclosed structures using radar are challenged, amongst other factors, by the presence of clutter caused by the EM scattering from the exterior front wall [1], [2]. Front wall return is typically stronger than that from targets of interest, such as humans. Further, wall reverberations introduce ringing in the radar range profiles, thereby obscuring the weak indoor target returns. Therefore, wall reflections need to be suppressed, prior to image formation.

A simple and effective method for wall clutter mitigation is background subtraction. However, access to empty scene measurements is not available in many applications. For conventional imaging using full data volume, three main approaches have been proposed for suppression of wall reflections without relying on the background scene data [3]-[7]. In the first approach, the front wall parameters, such as thickness and dielectric constant, are estimated from the first wave arrivals [3]. The estimated parameters can be used to model EM wall returns, which are subsequently subtracted from the total radar returns, rendering wall-free signals. Although this scheme is effective, it requires a calibration step, which involves measuring the radar return from a metal plate at the same standoff distance as the front wall under similar, if not identical, operating conditions [8]. The second approach applies a spatial filtering method for wall clutter mitigation, which relies on the invariance of wall returns with changing antenna location [4], [5]. The third approach recognizes the wall reflections as the strongest component of radar returns, in addition to its spatial invariance property. By applying singular value decomposition (SVD) to the measured data matrix, the wall returns are captured by the singular vectors associated with the dominant singular values and removed by orthogonal subspace projection [6], [7].

Recently, it has been shown that compressive sensing (CS) techniques can be applied, in lieu of backprojection, to reveal the target positions behind walls [9]-[11]. In so doing, significant savings in data acquisition time can be achieved. Further, producing an image of the indoor scene using few observations can be logistically important, as some of the data measurements in space and frequency can be difficult to attain. Both SVD- and spatial filtering-based wall mitigations in conjunction with CS were considered in [12]. Direct application of these methods to the reduced data volume was shown to provide satisfactory performance when the same subset of frequencies was used for each antenna in physical or synthetic aperture arrays. For the case where the frequencies were allowed to differ from one antenna to another, individual range profiles were first reconstructed using l_1 norm minimization employing a Fourier basis. Then, the data of the missing frequencies were obtained by taking the Fourier Transform of the reconstructed range profile at each antenna. Once the radar returns corresponding to all original frequencies were estimated, any conventional wall mitigation method could be applied. However, since the presence of the wall clutter renders each range profile quite dense, wall clutter mitigation was accomplished at the expense of target-to-clutter ratio compared to the case where the same set of reduced frequencies was employed at each available antenna location.

In this paper, we propose an alternate scheme to overcome the shortcomings of the wall clutter mitigation scheme proposed in [12] when different sets of reduced frequencies are used at the available antennas. We employ a dictionary based on discrete prolate spheroidal sequences (DPSS's) to represent the wall return and use a block sparse approach to capture and subsequently remove the wall clutter at each available antenna individually under reduced data volume. This permits the application of CS techniques for image reconstruction. Note that this scheme is also applicable to the case where the same set of reduced frequencies is used at each available antenna.

The paper is organized as follows. Section 2 briefly reviews DPSS's. Through-the-wall signal model is described in Section 3. The DPSS based wall clutter suppression scheme is presented in Section 4. CS based image reconstruction using the wall-suppressed data is described in Section 5. Supporting experimental results are presented in Section 6. Section 7 provides the conclusion.

2. DISCRETE PROLATE SPHEROIDAL SEQUENCES

DPSS's are a collection of index-limited sequences that maximize the energy concentration within a given frequency band [13], [14]. The DPSS's constitute a basis for finite-energy signals that are time-limited with their energy concentrated in a given bandwidth. In this paper, since we consider a stepped-frequency signal consisting of K frequencies, we deal with the dual problem to the conventional DPSS's. That is, we seek frequency domain sequences, $s[k]$, confined to the frequency index set $[0,1,\ldots,K-1]$, whose energy is concentrated in a finite normalized time interval $[-T, T)$, where $0 < T < 1/2$. The K-length frequency domain DPSS's are defined as solutions of [14]

$$As_i = \lambda_i s_i, \qquad i = 0,1,\cdots,K-1 \qquad (1)$$

where s_i is a $K \times 1$ vector with elements $s_i[k], k = 0,1,\cdots,K-1$, and λ_i are the eigenvalues of the matrix A, which is given by

$$[A]_{i,k} = \frac{\sin(2\pi T(i-k))}{\pi(i-k)}. \qquad (2)$$

The DPSS's are orthonormal on the set $\{0,1,\cdots,K-1\}$.

3. THROUGH-THE-WALL SIGNAL MODEL

Consider an M-element linear synthetic aperture radar located parallel to a homogeneous wall at a nonzero standoff distance. The radar employs a wideband stepped-frequency signal, consisting of K uniformly spaced frequencies $\{f_k\}_{k=0}^{K-1}$. Assuming monostatic operation, the wall return at the mth antenna location corresponding to the kth frequency is given by [1]

$$z_m^w(f_k) = \sum_{l=0}^{L} \sigma_w a_l \exp(-j2\pi f_k \tau_w^{(l)}) \qquad (3)$$

where σ_w is the complex wall reflectivity, L is the number of wall reverberations, $\tau_w^{(0)}$ is the propagation delay associated with the direct wall return, $\tau_w^{(l)}, l > 0$ are the delays associated with the wall reverberations, and a_l is the path loss associated with the lth wall return.

The return at the mth antenna corresponding to the kth frequency from P point targets behind the wall can be expressed as [1], [15]

$$z_m^t(f_k) = \sum_{p=0}^{P-1} \sigma_p \exp(-j2\pi f_k \tau_{p,m}) \qquad (4)$$

where σ_p is the complex reflectivity of the pth target, and $\tau_{p,m}$ is the two-way traveling time between the pth target and the mth antenna. Thus, the total baseband signal received by the mth antenna corresponding to the kth frequency is the superposition of the wall and target returns,

$$z_m(f_k) = z_m^w(f_k) + z_m^t(f_k) \qquad (5)$$

The signal received by the mth antenna at the K frequencies can be arranged into a $K \times 1$ vector z_m as

$$z_m = [z_m(f_0) \quad z_m(f_1) \quad \cdots \quad z_m(f_{K-1})]^T = z_m^w + z_m^t \quad (6)$$

with z_m^w, z_m^t representing the wall and target contribution vectors at the mth antenna, respectively.

4. DPSS-BASED WALL CLUTTER MITIGATION UNDER REDUCED DATA VOLUME

The Fourier transform of each of the $K \times 1$ received stepped-frequency signals $\{z_m\}_{m=0}^{M-1}$ is an ensemble of returns, each of duration $\frac{1}{f_{K-1}-f_0}$, concentrated on a number of time intervals within $\left[-\frac{1}{2\Delta f}, \frac{1}{2\Delta f}\right), \Delta f = \frac{f_{K-1}-f_0}{K-1}$. We refer to such signals as "multi-duration signals". We first construct a basis using DPSS's for efficiently capturing the structure of such signals.

4.1. DPSS Basis

We divide the unambiguous time $\left[-\frac{1}{2\Delta f}, \frac{1}{2\Delta f}\right)$ into $N = \left\lfloor \frac{2}{\Delta f D} - 1 \right\rfloor$ overlapping intervals of length $D = \frac{1}{f_{K-1}-f_0}$. Note that the choice of non-overlapping set of intervals would be inadequate since the radar returns from the various targets may not lie exactly on the grid. The nth time interval has an extent $\Delta_n = \left[-\frac{1}{2\Delta f} + \frac{nD}{2} - \frac{D}{2}, -\frac{1}{2\Delta f} + \frac{nD}{2} + \frac{D}{2}\right], n = 1,2,\cdots,N$. Let $T = \frac{D\Delta f}{2}$ and $t_n = \left(-\frac{1}{2\Delta f} + \frac{nD}{2}\right)\Delta f$. Consider the $K \times K$ matrix $S_{K,T}$ of K-length frequency domain DPSS's

$$S_{K,T} = [s_0 \quad s_1 \quad \ldots \quad s_{K-1}] \tag{7}$$

with $\{s_i\}_{i=0}^{K}$ defined in (1). Forming the $K \times K$ diagonal matrix E_{t_n} as

$$E_{t_n} = \begin{bmatrix} 1 & 0 & \ldots & 0 \\ 0 & e^{-j2\pi t_n} & \ldots & 0 \\ \vdots & \vdots & \ddots & \vdots \\ 0 & 0 & \ldots & e^{-j2\pi(K-1)t_n} \end{bmatrix}, \tag{8}$$

we can define the time-shifted DPSS basis for Δ_n as $E_{t_n} S_{K,T}$. It can be readily shown that $E_{t_n} S_{K,T}$ forms an orthonormal basis for the signals supported on Δ_n in $\mathbb{C}^K$. Further, the first $\lceil 2KT \rceil + 1$ time-shifted DPSS's suffice as the signal basis [16]. Therefore, we consider the $K \times (\lceil 2KT \rceil + 1)$ matrix Ψ_n, comprising the first $\lceil 2KT \rceil + 1$ columns of $E_{t_n} S_{K,T}$, as an efficient basis for signals supported on Δ_n. Thus, the $K \times (\lceil 2KT \rceil + 1)N$ DPSS basis Ψ for the multi-duration signals can be defined as the concatenation of the N time-shifted DPSS bases [16],

$$\Psi = [\Psi_1 \quad \Psi_2 \quad \ldots \quad \Psi_N]. \tag{9}$$

Using the DPSS basis Ψ, the received signal at the mth antenna can be expressed as

$$z_m = z_m^w + z_m^t = \Psi \rho_m^w + \Psi \rho_m^t, \ m = 0,1,\ldots, M-1 \tag{10}$$

where ρ_m^w and ρ_m^t are the $(\lceil 2KT \rceil + 1)N$-length coefficient vectors corresponding to the wall and target returns, respectively. It is noted that because of the multi-duration nature of the radar returns, the wall and target contributions z_m^w, z_m^t can be represented using only the columns of Ψ corresponding to the occupied time intervals. As a result, both ρ_m^w and ρ_m^t exhibit a block-sparse structure, i.e. the nonzero coefficients cluster in a small number of blocks.

4.2. Wall Clutter Mitigation under Reduced Data Volume

The data model in (10) involves the full set of measurements made at all M antenna locations using the K frequencies. Assume only $M_1 (< M)$ randomly selected antenna locations are available for data collection. Let $i_g \in [0,1,\ldots,M-1]$, for $g = 0,1,\ldots,M_1-1$, be the indices of the employed antenna locations. Consider $\breve{z}_{i_g}$, which is a vector of length $K_1 \ll K$, consisting of elements chosen from z_{i_g} as follows.

$$\breve{z}_{i_g} = \varphi^{(g)} z_{i_g} = \varphi^{(g)} z_{i_g}^w + \varphi^{(g)} z_{i_g}^t = \breve{z}_{i_g}^w + \breve{z}_{i_g}^t$$
$$= \varphi^{(g)} \Psi \rho_{i_g}^w + \varphi^{(g)} \Psi \rho_{i_g}^t \tag{11}$$

where $\varphi^{(g)}$ is a $K_1 \times K$ measurement matrix constructed by randomly selecting K_1 rows of a $K \times K$ identity matrix. The matrix $\varphi^{(g)}$ determines the reduced set of frequencies corresponding to the i_gth antenna location.

The goal is to reconstruct the wall contribution at each employed antenna location individually using the reduced measurement vector $\breve{z}_{i_g}$, which can then be subtracted from $\breve{z}_{i_g}$ to obtain the clutter-free radar return at the i_gth antenna. Because of the block sparse nature of $\rho_{i_g}^w$ and $\rho_{i_g}^t$, we use the block extension of orthogonal matching pursuit (BOMP) to recover the wall component [17]. As previously stated, the wall return is stronger than the target returns and dominates the energy in the data. Also, in practice, due to the strong attenuation in wall materials, only one to two wall reverberation responses are typically observed [18]. Therefore, the first two to three BOMP iterations will capture the wall contribution [19]. This implies that the output of the BOMP algorithm $\hat{z}_{i_g} \approx \breve{z}_{i_g}^w$. Thus, the target contribution can be obtained by simply subtracting the reconstructed wall contribution,

$$\breve{z}_{i_g} - \hat{z}_{i_g} \approx \breve{z}_{i_g}^t \tag{12}$$

Once the wall clutter has been suppressed individually at each employed antenna location, we can proceed with image formation under reduced data volume.

5. CS BASED IMAGE FORMATION

Assume that the scene being imaged is divided into $N_x \times N_y$ pixels in crossrange and downrange. Vectorizing the image into an $N_x N_y \times 1$ scene reflectivity vector σ and using the wall-free signal model in (4), we obtain the linear system of equations,

$$\breve{z}_{i_j}^t = \Theta_{i_j} \sigma. \tag{13}$$

The rth element of the qth column of the $K_1 \times N_x N_y$ matrix Θ_{i_g} is given by

$$\left[\Theta_{i_g}\right]_{r,q} = \exp\left(-j2\pi f_r \tau_{i_g,q}\right), \ r = 0,1,\ldots,K_1-1,$$
$$q = 0,1,\ldots,N_x N_y - 1 \tag{14}$$

where $\tau_{i_g,q}$ is the two-way traveling time between the qth pixel and the i_gth antenna. The vector σ in (13) is a weighted indicator vector defining the scene reflectivity, i.e., if there is a target at the qth pixel, then the value of the qth element of σ equals the target reflectivity. Otherwise, it is zero. Stacking the wall-free signal samples from all M_1 antenna elements, we obtain the $M_1 K_1 \times 1$ measurement vector $\breve{z}^t$ as

$$\breve{z}^t = \Theta \sigma \tag{15}$$

where $\Theta = \left[\Theta_{i_0}^T \quad \Theta_{i_1}^T \quad \cdots \quad \Theta_{i_{(M_1-1)}}^T\right]^T$. Given the reduced measurement vector $\breve{z}^t$ in (15), we can recover σ by solving the following l_1 norm minimization problem,

$$\hat{\sigma} = \arg\min_{\sigma} \|\sigma\|_1, \ \text{subject to } \breve{z}^t \approx \Theta \sigma \tag{16}$$

The problem in (16) can be solved using convex relaxation, greedy pursuit, or combinatorial algorithms. In this work, we use OMP for the CS based reconstruction [20].

6. EXPERIMENTAL RESULTS

In this section, we present results of the DPSS based scheme and provide performance comparison with the wall-mitigation based CS approach proposed in [12] for the case of having different sets of reduced frequency measurements at different available antenna locations.

A stepped-frequency synthetic aperture radar system was used to perform real through-the-wall measurements in the Radar Imaging Lab at Villanova University. The synthetic linear aperture consisted of 67 uniformly spaced elements, with an inter-element spacing of 0.0187 m. The aperture was located parallel to a 0.14 m thick solid concrete wall at a standoff distance of 1.24 m. The stepped-frequency signal comprised 728 frequencies from 1 to 3 GHz, with a step size of 2.75MHz. A vertical metal dihedral, located at (0, 4.4) m, was used as the target. Each face of the dihedral was 0.39 m × 0.28 m. The back and the side walls were covered with RF absorbing material. Measurements from the empty scene without the target were also made.

The scene to be imaged is chosen to be 4 m × 6 m centered at (0, 3) m and divided into 41×36 pixels. Figure 1(a) shows the l_1 norm reconstructed image corresponding to the measured scene using the full raw dataset. OMP was used for image formation. The number of OMP iterations, usually associated with the scene sparsity, was set to 100 in this case. In this and all subsequent images, we plot the image intensity on a 35 dB scale, with the maximum intensity value in each image normalized to 0 dB. We notice the strong antenna ringing present in the data, showing up in the image at downranges prior to the front wall. Since the target return is much weaker than the antenna ringing and the wall return, only the antenna ringing and wall have been reconstructed and the algorithm fails to detect the target. With the availability of empty scene measurements, we can perform background subtraction to remove antenna ringing and wall clutter. The target is clearly visible in the corresponding l_1 norm reconstructed image using full data volume, shown in Fig. 1(b). The number of OMP iterations was chosen to be 5 in this case. Note that there is a slight bias in the imaged target location. This is because we do not correct for the additional propagation delay encountered by the signal as it travels through the wall.

Next, we randomly selected 20% of antenna locations and randomly chose 20% of frequencies at each selected antenna location. Figure 2(a) shows the l_1 norm reconstructed image with 5 OMP iterations after the proposed DPSS based wall clutter mitigation. In order to effectively capture the antenna ringing and the front wall contributions, the number of BOMP iterations was set to 11. Clearly, the DPSS based scheme successfully removed both the antenna ringing and the wall, thereby allowing the

subsequent l_1 norm image reconstruction to locate the target. For the wall clutter mitigation scheme of [12], we first recovered all the frequency measurements at each employed antenna location through l_1 norm range profile reconstruction using the Fourier basis. The number of OMP iterations for the individual range profile reconstructions was set to 120. Figure 2(b) shows the reconstructed image after applying subspace projection based wall mitigation scheme to the full frequency data recovered from the reconstructed range profiles. We observe that the target is barely localized and there are substantial antenna ringing and wall clutter residuals visible in the image.

7. CONCLUSION

We presented a DPSS based wall clutter rejection scheme for imaging of stationary targets behind walls using reduced data volume. First, the DPSS basis was used to effectively capture the energy of the wall return at each employed antenna. The reconstructed wall return was subtracted from the measured data at each individual antenna to obtain the wall-free measurements. This enabled the application of CS techniques for scene reconstruction with fewer observations. Supporting results based on real data experiments demonstrated the performance of the proposed scheme for the case when the reduced sets of frequency measurements were allowed to vary from one antenna to the other.

ACKNOWLEDGMENT

REFERENCES

[1] M. Amin (Ed.), *Through-the-Wall Radar Imaging*, CRC Press, Boca Raton, FL, 2010.

[2] P. Chang, R. Burkholder, J. Volakis, R. Marhefka, and Y. Bayram, "High-frequency EM characterization of through-wall building imaging," *IEEE Trans. Geosci. Remote Sens.*, vol. 47, no. 5, pp. 1375–1387, 2009.

[3] M. Dehmollaian and K. Sarabandi, "Refocusing through building walls using synthetic aperture radar," *IEEE Trans. Geosci. Remote Sens.*, vol. 46, pp. 1589–1599, 2008.

[4] Y. Yoon and M. Amin, "Spatial filtering for wall-clutter mitigation in through-the-wall radar imaging," *IEEE Trans. Geosci. Remote Sens.*, vol. 47, no. 9, pp. 3192–3208, 2009.

[5] M. Dehmollaian, M. Thiel, and K. Sarabandi, "Through-the-wall imaging using differential SAR," *IEEE Trans. Geosci. Remote Sens.*, vol. 47, no. 5, pp. 1289-1296, 2009.

[6] A. Chandra, D. Gaikwad, D. Singh, and M. Nigam, "An approach to remove the clutter and detect the target for ultra-wideband through-wall imaging," *J. Geophysics and Engineering*, vol. 5, no. 4, pp. 412–419, 2008.

[7] F. Tivive, A. Bouzerdoum, and M. Amin, "An SVD-based approach for mitigating wall reflections in through-the-wall radar imaging," in *Proc. IEEE Radar Conf.*, Kansas City, MO, May, 2011, pp. 519–524.
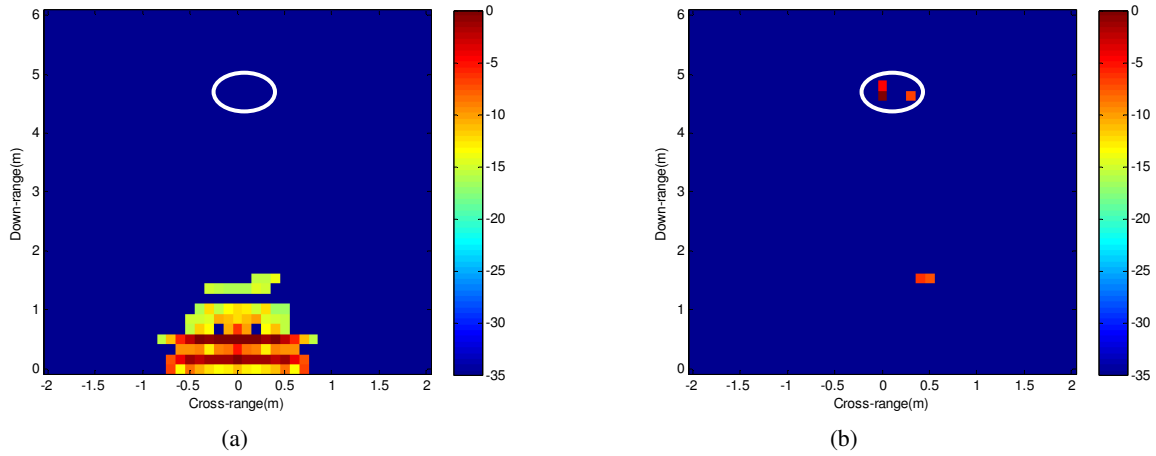
Figure 1. l_1 norm reconstructed images with full data volume, (a) no preprocessing, (b) after background subtraction.
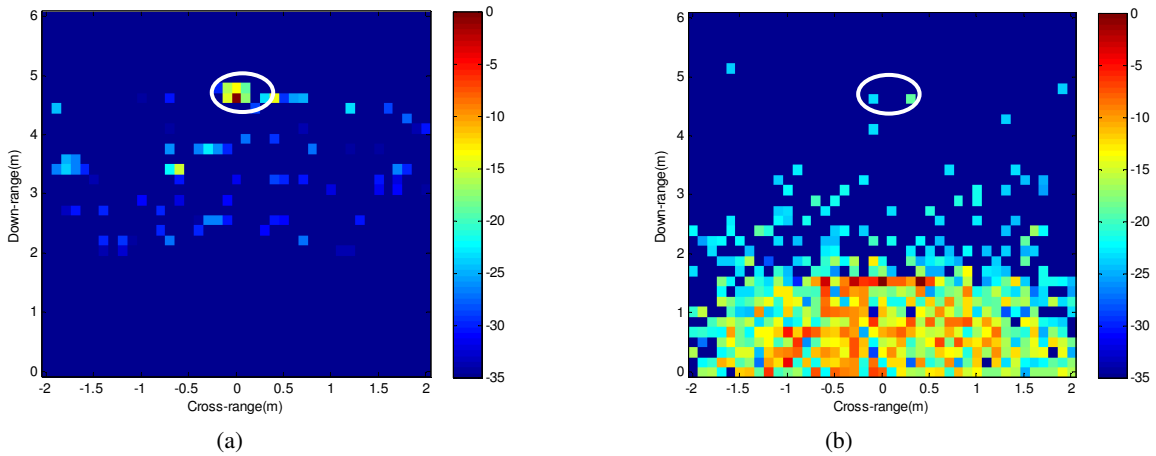
Figure 2. l_1 norm reconstructed images after wall clutter mitigation, (a) proposed DPSS based approach, (b) wall clutter mitigation proposed in [11]. Target position is indicated by the white circle in each image.

[8] M. Aftanas, J. Sachs, M. Drutarovsky, and D. Kocur, "Efficient and fast method of wall parameter estimation by using UWB radar system," *J. Frequenz*, vol. 63, pp. 231–235, 2009.

[9] Y. Yoon and M. Amin, "Compressed sensing technique for high-resolution radar imaging," in *Proc. SPIE*, vol. 6968, 2008, pp. 69681A–1–69681A–10.

[10] Q. Huang, L. Qu, B. Wu, and G. Fang, "UWB through-wall imaging based on compressive sensing," *IEEE Trans. Geosci. Remote Sens.*, vol. 48, no. 3, pp. 1408-1415, 2010.

[11] M. Leigsnering, C. Debes, and A. Zoubir, "Compressive sensing in through-the-wall radar imaging," in *Proc. IEEE ICASSP*, Prague, Czech Republic, 2011, pp. 4008–4011.

[12] E. Lagunas, M. Amin, F. Ahmad, and M. Najar, "Joint wall mitigation and compressive sensing for indoor image reconstruction," *IEEE Trans. Geosci. Remote Sens.*, vol. 51, no. 2, pp. 891-906, 2013.

[13] D. Slepian, "Prolate spheroidal wave functions, Fourier analysis, and uncertainty. V – The discrete case," *Bell Syst. Tech. J.* , vol. 57, no. 5, pp. 1371–1430, 1978.

[14] T. Zemen and C. Mecklenbräuker, "Time-variant channel estimation using discrete prolate spheroidal sequences," *IEEE Trans, Signal Process.*, vol. 53, No. 9, pp. 3597-3607, 2005.

[15] M. Amin and F. Ahmad, "Wideband synthetic aperture beamforming for through-the-wall imaging," *IEEE Signal Process. Mag.*, vol. 25, no. 4, pp. 110-113, 2008.

[16] M. Davenport and M. Wakin, "Compressive sensing of analog signals using discrete prolate spheroidal sequences," *Applied and Computational Harmonic Analysis*, vol. 33, no. 3, pp. 438-472, 2012.

[17] Y. Eldar, P. Kuppinger, and H. Bolcskei, "Block-sparse signals: uncertainty relations and efficient recovery," *IEEE Trans. Signal Process.*, vol. 58, no. 6, pp. 3042–3054, 2010.

[18] C. Thajudeen, A. Hoorfar, F. Ahmad, and T. Dogaru, "Measured complex permittivity of walls with different hydration levels and the effect on power estimation of TWRI target returns," *Progress in Electromagnetic Research B*, vol. 30, pp. 177–199, 2011.

[19] J. Tropp, A. Gilbert, and M. Strauss, "Algorithms for simultaneous sparse approximation. Part I: Greedy pursuit," *Signal Processing*, vol. 86, no. 3, pp. 572-588, 2006.

[20] J. Tropp and A. Gilbert, "Signal recovery from random measurements via orthogonal matching pursuit," *IEEE Trans. Inf. Theory*, vol. 53, no. 12, pp. 4655–4666, 2007.